Effects of Inhomogeneous Cloud Properties on 2-D Longwave Radiative Transfer

T. C. Benner, J. A. Curry, and K. F. Evans
Program in Atmospheric and Oceanic Sciences
University of Colorado
Boulder, Colorado

Introduction

Clouds have a profound influence on radiative fluxes, for both solar and infrared radiation. Inhomogeneous clouds, in particular, have complex effects on fluxes and can be challenging to parameterize. Killen and Ellingson (1994) showed the importance of cloud geometry and spatial distribution on infrared fluxes, while Takara and Ellingson (1996) emphasized the necessity of modeling both cloud geometry and scattering to obtain accurate longwave fluxes. Both these studies point to the need for a thorough understanding of the radiative effects of inhomogeneous clouds. This study used the Spherical Harmonics Discrete Ordinate Method (SHDOM) radiative transfer model with three sets of large eddy simulation (LES) output to explore the effects of inhomogeneous clouds on infrared fluxes, including the errors produced by common approximations compared to a full solution.

Model

This study used the SHDOM radiative transfer model (Evans 1998). This model represents radiation explicitly via spherical harmonics. It integrates the radiative transfer equation along discrete ordinates through a spatial grid to model the streaming of radiation. It uses a type of successive order of scattering approach. It computes accurate radiances or fluxes in either the shortwave or longwave, even for highly peaked phase functions. It computes broadband radiative transfer with a correlated k-distribution. The SHDOM model accommodates many detailed inputs, including atmospheric properties (T, P, p, pv, O3, CO_2, CH_4, N_2O), cloud properties (LWC, N, reff, a, phase), and surface properties (T, e, a, Mre, Mim).

Model Inputs

This study used output from three LESs, based on different atmospheric conditions, as input to the SHDOM radiative transfer model. This included liquid water content (LWC) fields and soundings of temperature, pressure, density, and water vapor. Each case used a two-dimensional (2-D) slice from three-dimensional (3-D) output and assumed a homogeneous emitting ocean surface. The first case was a stratocumulus cloud deck based on conditions observed during the First International Satellite Cloud Climatology Program (ISCCP) Regional Experiment (FIRE) (Moeng et al. 1996). This experiment took place in the midlatitude Pacific Ocean southwest of California in the summer of 1987. Figure 1 shows the LWC field and the liquid water path (LWP) for the 2-D slice from this case used in this study. The second case was a stratus-topped atmospheric boundary layer (ABL) derived from typical conditions in the maritime midlatitudes (Kosovic 1998, personal communication). The third case was a field of small cumulus clouds

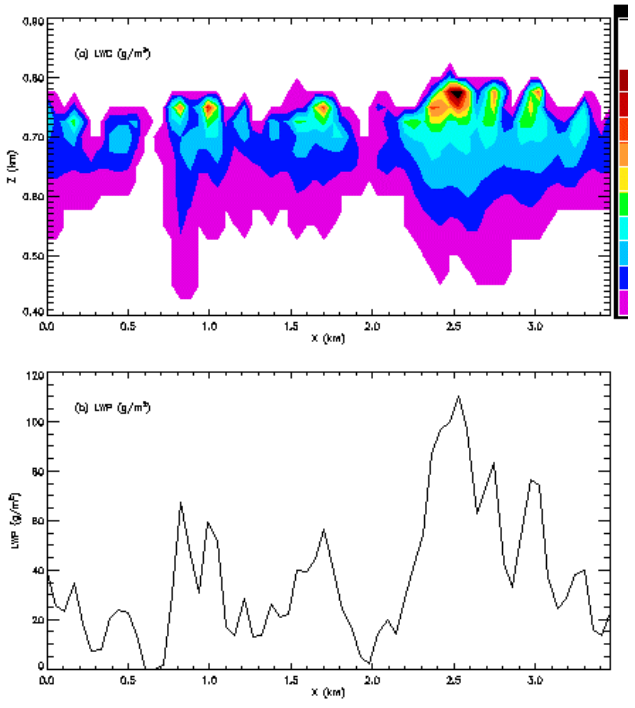

Figure 1. LWC and LWP for the 2-D slice of the FIRE LES output. (For a color version of this figure, please see *http://www.arm.gov/docs/documents/technical/conf_9803/benner-98.pdf*.)

based on conditions observed during the Barbados Oceanographic and Meteorological Experiment (BOMEX). This experiment took place in the tropical Atlantic Ocean east of Barbados in the summer of 1969.

Model Runs

For each of the three LES cases, the model was run several times to explore different sensitivities. It was run in both broadband and monochromatic (10-micron) infrared. Broadband runs included gaseous absorption in 12 bands (Fu and Liou 1992). It was run in 2-D mode and in independent pixel approximation (IPA) mode. It was also run on two columns (clear and domain average cloudy), combined and weighted by the cloud fraction for a plane parallel computation. Fluxes were calculated above the cloud layer (upwelling) and at the surface (downwelling). Model runs used a liquid water droplet concentration N = 100 cm^{-3}, a gamma distribution of 50 effective radii ranging from 0.5 to 25.0 microns, with a shape parameter alpha = 7, and an ocean surface with an emissivity e = 0.98 and a surface temperature equal to that of the lowest atmospheric level.

Results - Fluxes

Model runs gave distributions of infrared flux along the 2-D LES output. Fluxes for the FIRE LES case appear in Figure 2. As shown by the difference between the 2-D radiative transfer calculations (left side) and the IPA (right side), the inhomogeneous clouds produced striking 2-D effects. In the upwelling fluxes above the cloud layer (e.g., Figure 2a), the highest flux values were above gaps in the clouds, through which radiation from the warm surface could penetrate, and above the thickest part of the cloud at 2.5 km, where the top of the cloud reached into the inversion and was only slightly cooler than the surface. Low flux values corresponded to moderately thick parts of the cloud at cooler temperatures. In the downwelling fluxes at the surface, the highest flux values were below the thicker parts of the cloud, which radiated at atmospheric temperature. The lowest values were below gaps in the clouds, through which the surface could see the cold sky. There was more variation in flux values for the IPA than for the 2-D calculation (e.g., Figure 2b versus Figure 2a), since in the latter case the horizontal transfer of radiation could smooth the distribution. There was also more variation for downwelling fluxes than upwelling fluxes (e.g., Figure 2c versus Figure 2b), because of the very cold sky assumed in the model runs. Downwelling fluxes appeared very similar for either broadband or 10-micron runs, for either 2-D calculations (Figures 2c and 2g) or the IPA (Figures 2d and 2h).

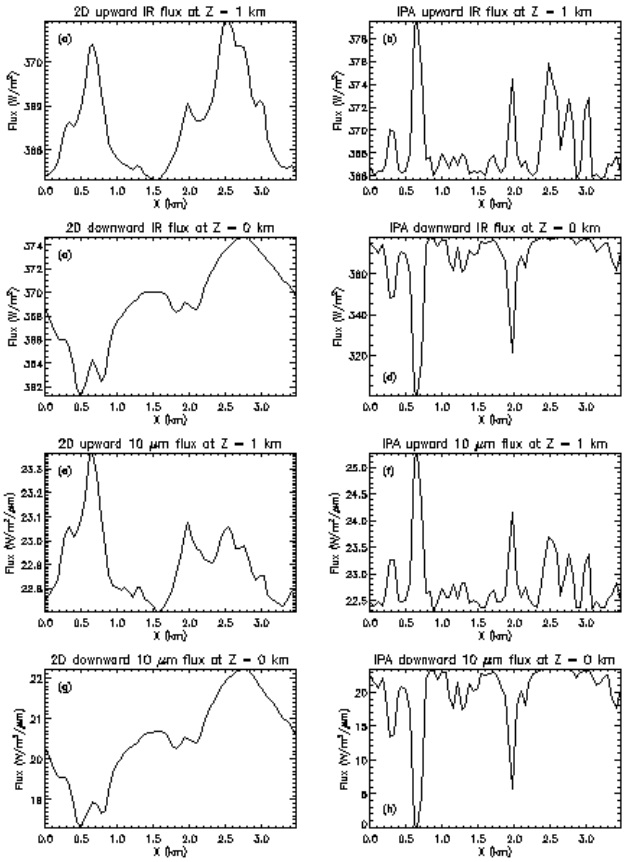

Figure 2. Upward and downward infrared fluxes for the FIRE LES case, using both broadband and monochromatic radiation, for full 2-D radiative transfer and the IPA.

The minimum flux value reached zero under the gap in the clouds at 0.65 km for the 10-micron IPA run (Figure 2h) due to the assumed cold sky. It never reached zero in the other downwelling results due to emission by absorbing gases (Figure 2d), 2-D effects (Figure 2g), or both (Figure 2c). For both 2-D calculations and the IPA, the thickest part of the cloud made a greater impact on upwelling fluxes for broadband runs than for 10-micron runs. In the 2-D case, the absorbing gases in the broadband run (Figure 2a) prevented more of the radiation from escaping to the sides, compared to the 10-micron run (Figure 2e). In the IPA case, the effect is not as great, resulting again from gaseous absorption. Without the absorbing gases (Figure 2f), radiation from the thickest part of the cloud streamed upward unhindered. In the broadband case (Figure 2b), however, radiation was absorbed above the cloud at the peak of the cloud top inversion, then reradiated at a higher temperature, resulting in a greater flux.

Domain average fluxes were also computed, and those for the IPA and plane parallel calculations were compared to the corresponding 2-D calculations to determine the size of the resulting error. These appear in Table 1. The IPA was found to be highly accurate for domain average fluxes, except for monochromatic fluxes at the surface. The plane parallel approximation was also found to be reasonably accurate. For the FIRE LES case, it produced larger errors than the IPA for all runs. For the other two cases, however, it produced larger errors for upwelling fluxes above the cloud layer and smaller errors for downwelling fluxes at the surface. In all cases, downwelling fluxes at the surface were subject to larger errors than upwelling fluxes above the cloud layer. Also in all cases, the errors in the broadband runs were smaller than those in the corresponding 10-micron runs, indicating that gaseous absorption is important for the proper representation of radiative transfer in a cloudy boundary layer.

Results - TKE

For the FIRE LES case, the heating rate (h') was output from SHDOM, and the vertical velocity (w') was taken from the original LES output. These were combined and averaged at each level to obtain profiles of w'h' in the cloud layer for both 2-D and IPA radiative transfer. w'h' is part of the buoyancy production term in the turbulent kinetic energy (TKE) equation. In a cloudy atmospheric boundary layer, it is very important for TKE production, especially at cloud top. Figure 3 shows that w'h' differed appreciably between the two methods for the lower part of the cloud top. This corresponds to wells in the top of the cloud, where radiation from surrounding higher regions offsets the cloud top radiative cooling, thus reducing the negative buoyancy and the production of TKE. w'h' also differs somewhat for the upper part of the cloud top, corresponding to higher turrets. These turrets receive less radiation from nearby parts of the cloud top and can radiate freely, so TKE production is enhanced. These effects appear in the 2-D representation but not in the IPA. This suggests that IPA may not be adequate for computing w'h' in inhomogeneous clouds.

Conclusions

This study examined the transfer of radiation through 2-D slices of three simulated cloudy boundary layers. The IPA is highly accurate for domain average broadband infrared fluxes, but it can produce significant errors for monochromatic infrared fluxes at the surface. The plane parallel approximation is also accurate for domain average broadband infrared fluxes. In two of three cases, compared to the IPA, it produces smaller errors for upwelling fluxes above the cloud layer and larger errors for downwelling fluxes at the surface. Neither approximation is especially good at describing the spatial distribution of fluxes in a cloudy atmospheric boundary layer, which are strongly influenced by horizontal radiative transfer. Downwelling infrared fluxes at the surface are subject to larger errors than upwelling infrared fluxes above the cloud layer. By including gaseous absorption, the errors produced by either approximation are reduced. Significant errors in TKE production can result from heating rates derived using the IPA, particularly in the lower parts of the cloud top.

Table 1. Percent errors in domain average fluxes resulting from independent pixel and plane parallel approximations, compared to full 2-D calculations, including all three LES cases, broadband and monochromatic fluxes, and upwelling and downwelling fluxes.

		FIRE		**Midlatitude**		**BOMEX**	
		Broadband	**10 μm**	**Broadband**	**10 μm**	**Broadband**	**10 μm**
IPA	Up	-0.01	-0.13	+0.01	-0.28	+0.06	+0.07
	Down	-0.60	-3.78	-0.60	+17.06	-0.65	-23.10
PP	Up	-0.13	-0.96	-0.07	-0.53	-0.14	0.81
	Down	+1.67	+7.37	-0.25	+12.94	-0.13	+12.24

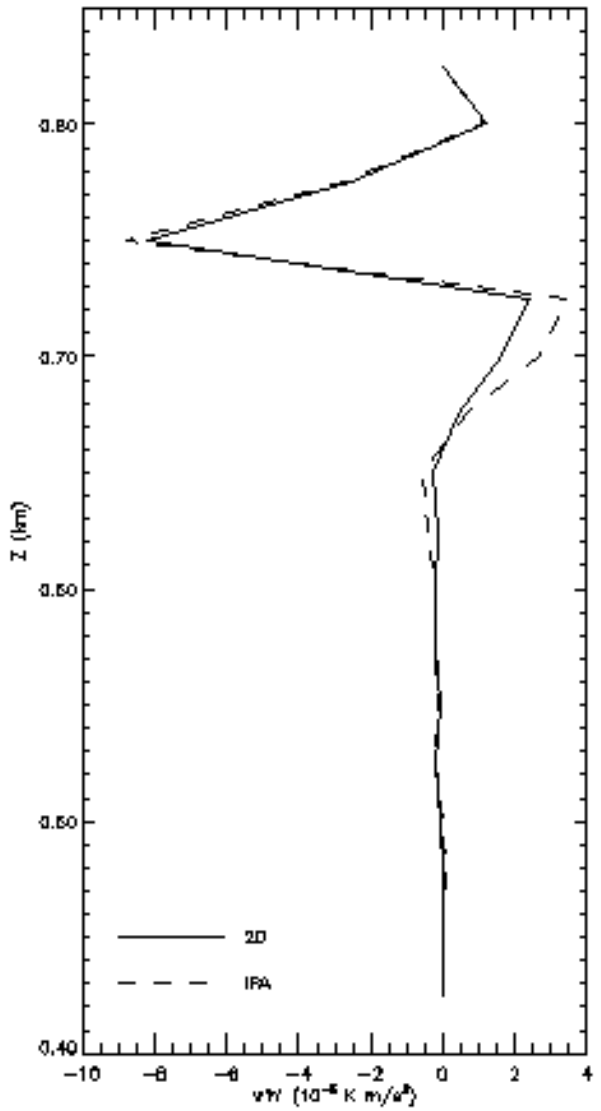

Figure 3. Profiles of level-average w'h' for the FIRE LES case, for both 2-D radiative transfer and the independent pixel approximation.

References

Evans, K. F., 1998: The spherical harmonics discrete ordinate method for three-dimensional radiative transfer. *J. Atmos. Sci*., **55**, 429-446.

Fu, Q., and K. N. Liou, 1992: On the correlated k-distribution method for radiative transfer in inhomogeneous atmospheres. *J. Atmos. Sci*., **49**, 2139-2156.

Killen, R. M., and R. G. Ellingson, 1994: The effect of shape and spatial distribution of cumulus clouds on longwave irradiance. *J. Atmos. Sci*., **51**, 2123-2136.

Moeng, C.-H., W. R. Cotton, C. Bretherton, A. Chlond, M. Khairoutdinov, S. Krueger, W. S. Lewellen, M. K. MacVean, J.R.M. Pasquier, H. A. Rand, A. P. Siebesma, B. Stevens, and R. I. Sykes, 1996: Simulations of a stratocumulus-topped planetary boundary layer: Intercomparisons among different numerical codes. *Bull. Amer. Meteor. Soc*., **77**, 261-278.

Takara, E. E., and R. G. Ellingson, 1996: Scattering effects on longwave fluxes in broken cloud fields. *J. Atmos. Sci*., **53**, 1464-1476.